JACS
JOURNAL OF THE AMERICAN CHEMICAL SOCIETY
Communication
pubs.acs.org/JACS

Evidence of Highly Active Cobalt Oxide Catalyst for the Fischer–Tropsch Synthesis and CO_2 Hydrogenation

Gérôme Melaet,[†,‡] Walter T. Ralston,[†,‡] Cheng-Shiuan Li,[†,§] Selim Alayoglu,*[,†,§] Kwangjin An,[†,§] Nathan Musselwhite,[†,‡] Bora Kalkan,[⊥] and Gabor A. Somorjai*[,†,§]

[†]Department of Chemistry, University of California, Berkeley, California 94720, United States
[‡]Chemical Science Division, [§]Materials Sciences Division, and [⊥]Advanced Light Source, Lawrence Berkeley National Laboratory, Berkeley, California 94720, United States

Supporting Information

ABSTRACT: Hydrogenations of CO or CO_2 are important catalytic reactions as they are interesting alternatives to produce fine chemical feedstock hence avoiding the use of fossil sources. Using monodisperse nanoparticle (NP) catalysts, we have studied the CO/H_2 (i.e., Fischer–Tropsch synthesis) and CO_2/H_2 reactions. Exploiting synchrotron based *in situ* characterization techniques such as XANES and XPS, we were able to demonstrate that 10 nm Co NPs cannot be reduced at 250 °C while supported on TiO_2 or SiO_2 and that the complete reduction of cobalt can only be achieved at 450 °C. Interestingly, cobalt oxide performs better than fully reduced cobalt when supported on TiO_2. In fact, the catalytic results indicate an enhancement of 10-fold for the CO_2/H_2 reaction rate and 2-fold for the CO/H_2 reaction rate for the Co/TiO_2 treated at 250 °C in H_2 versus Co/TiO_2 treated at 450 °C. Inversely, the activity of cobalt supported on SiO_2 has a higher turnover frequency when cobalt is metallic. The product distributions could be tuned depending on the support and the oxidation state of cobalt. For oxidized cobalt on TiO_2, we observed an increase of methane production for the CO_2/H_2 reaction whereas it is more selective to unsaturated products for the CO/H_2 reaction. *In situ* investigation of the catalysts indicated wetting of the TiO_2 support by CoO_x and partial encapsulation of metallic Co by TiO_{2-x}.

Reforming of CO (i.e., Fischer–Tropsch (F–T) synthesis) and CO_2 to substitute dwindling fossil fuels has gained renewed scientific interest because of the recent crude oil crisis. The major drawback of these syntheses is their broad spectrum of products over Co catalysts: the hydrogenation of CO leads to formation of many high molecular weight products (C_5 and above), while CO_2 hydrogenation gives rise to gaseous products (i.e., C_1–C_4). Hence, both reactions represent a challenge to achieving 100% selectivity for a desired product. Accomplishing this will certainly enable "green" manufacturing with no generation of wasteful or polluting byproducts. Along these lines, studies of size-controlled Co particles showed that larger particles (i.e., ≥ 10 nm) are the most active, but size has a modest effect on the selectivity.[1−3] Likewise, TiO_2 supports were reported to enhance activity without altering selectivity.

The poor activity of smaller particles is often attributed to the ease with which these particles can be oxidized.[3,4] It is well-known from surface science that metallic Co is necessary to dissociate CO; hence, the metallic state is most likely to be the active state. In the present work, we report a cobalt oxide catalyst which is more active and more selective than its metallic equivalent. In fact, we observed multiple fold enhancement in turnover rates in the oxidized cubic CoO phase relative to metallic Co over the TiO_2 support. Inversely, metallic Co is more active when supported on SiO_2. Nevertheless, the CoO/TiO_2 performs better than the metallic Co/SiO_2 catalyst produced under the same conditions.

Since the nature of the support is known to influence the particle dispersion and size distribution while using classic impregnation techniques,[5] we have synthesized the particles using a colloidal route to ensure the homogeneity of cobalt size and dispersion between both catalysts. Cobalt nanoparticles (NPs) of 10 ±0.5 nm were synthesized using a colloidal method reported elswhere.[6] Macroporous TiO_2[7] and mesoporous SiO_2 (MCF-17)[8] were also prepared in-house and used as supports for the Co NPs.

We evaluated the catalytic activity and selectivity of Co/TiO_2 and Co/SiO_2 catalysts with metallic and oxidized Co components, as determined by the temperature of the reductive H_2 pretreatment. Two temperatures of hydrogen pretreatment were selected: one below the bulk reduction temperature of cobalt oxides (250 °C) and another above it (450 °C) respectively referred to as "ox" and "red", in order to evaluate the impact of the cobalt oxidation state. Both reactions were evaluated under similar temperature and pressure conditions (250 °C and ∼5 atm). Figure 1 exhibits plots of turnover frequencies (Figure 1a) and selectivity toward methane (Figure 1b) for the CO_2/H_2 (ratio 1:3) reaction, displaying four cycles of catalytic runs. We found that the Co/TiO_2 catalyst performed approximately 5-fold better when Co was in an oxidized state. Furthermore, methane production was improved substantially for the oxidized Co. We also found that the Co/SiO_2 catalyst behaved contrastingly to the Co/TiO_2 catalyst: peaks in activity and methane selectivity were obtained for the metallic Co. Overall, oxidized Co supported on TiO_2 displayed

Received: December 9, 2013
Published: January 24, 2014

   dx.doi.org/10.1021/ja412447q | *J. Am. Chem. Soc.* 2014, 136, 2260–2263

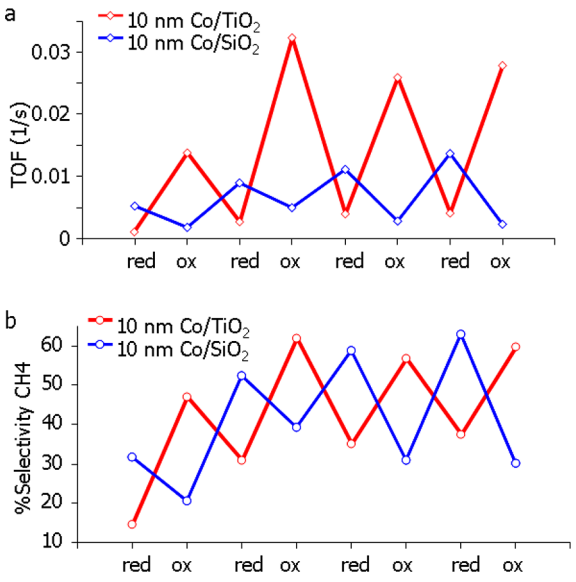

Figure 1. (a) TOFs and (b) % CH_4 selectivities for the Co/TiO_2 (red) and Co/SiO_2 (blue) catalysts as a function of the alternating redox state of Co; "red" stands for the reduced Co, and "ox" for the oxidized Co. The reduced Co was obtained upon H_2 treatment (20 vol % in He for 1 h) at 450 °C, while the oxidized Co was obtained upon O_2 treatment at 350 °C and maintained in net reducing atmospheres at 250 °C (see text). The reaction conditions were 5 atm of CO_2/H_2 (1:3) at 250 °C for 1 h.

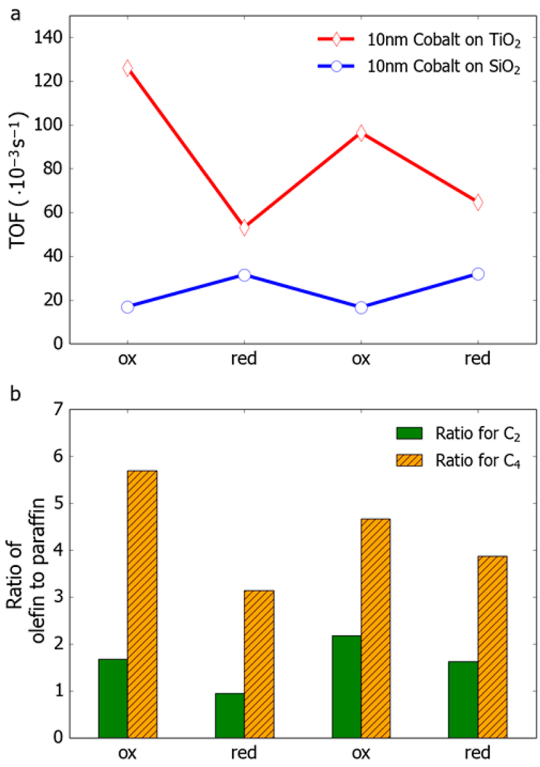

Figure 2. (a) TOFs for the Co/TiO_2 (red) and Co/SiO_2 (blue) catalysts as a function of alternating redox state of Co; "red" stands for the reduced Co, and "ox" for the oxidized Co. (b) Bar graph shows the olefin to paraffin ratios for C_2 and C_4 molecules for the Co/TiO_2 catalyst. The reduced Co was obtained upon H_2 treatment (10 vol % in Ar for 1 h) at 450 °C, while the oxidized Co was obtained upon O_2 treatment at 350 °C and maintained in net reducing atmospheres at 250 °C (see text). The reaction conditions were 5 atm of CO/H_2 (1:2) at 250 °C for 24 h.

a 2-fold enhancement in methane yield versus metallic Co supported on SiO_2.

Likewise, the CO/H_2 (ratio 1:2) reaction yielded 2-fold enhancement in turnover rates over oxidized Co in the case of TiO_2 support, whereas the Co/SiO_2 catalyst is most active with metallic Co (Figure 2a). Product distribution is also influenced by the oxidation state of cobalt. In fact for both supports, the oxidized cobalt produces more unsaturated hydrocarbons as shown for C_2 and C_4 in the case of the Co/TiO_2 catalyst (Figure 2b). Hence we can conclude that the hydrogenation activity of metallic cobalt is higher as we observe a diminishing of the olefin to paraffin ratio.

TEM, HR-TEM, and STEM/EDS spectral maps at Co and Ti K lines of the Co/TiO_x spent catalyst cycled at elevated temperatures (up to 450 °C) and reactive gas pressures (up to 5 bar) indicate no particle agglomeration (Figure S1a–e).

Figure 3 (a and b) shows AP-XPS spectra taken at Co and Ti 2p core levels during reductive H_2 (100 mTorr) treatments: at 250 °C, Co was found oxidized and Ti was partially reduced on surfaces corresponding to probing depths of 6 Å (kinetic energies of 180 eV),[9] whereas Co was partially reduced and Ti was fully reduced to Ti^{3+} at 450 °C. Under catalytically more relevant H_2 partial pressures (150 Torr), (N)EXAFS indicated metallic Co at 450 °C and oxidized Co at 250 °C (Figure 3c). EXAFS oscillations revealed metallic Co–Co coordination or Co–O and oxidized Co–Co coordination, respectively (Figure 3d).

Metallic Co is believed to be the active form of Co during hydrogenation of CO.[10,11] To this end, our findings over the Co/SiO_2 catalyst are in accord with an active metallic Co phase. However, we found evidence for the existence of an oxidized form of Co supported on TiO_2, surprisingly superior to the metallic state of Co for both the Fischer–Tropsch synthesis and for the hydrogenation of CO_2. A NEXAFS total electron yield (TEY) spectrum, a surface sensitive technique (probe depth ~2 nm), at the Co L edge revealed that near surface regions were composed of Co^{2+} during CO_2/H_2 (1:3, ~1 atm) reaction at 250 °C (Figure 3e). Furthermore, the C K edge TEY spectrum, obtained under the same reaction conditions, indicated the presence of CO and sp^2- and sp^3-like (i.e., C_2H_4 and CH_4) hydrocarbons[12] (Figure 3f). NEXAFS fluorescence yield (FY) spectra, acquired at the Co K edge under 1 atm of CO_2/H_2 (1:3) at 250 °C, demonstrate that the active cobalt oxide catalyst remained oxidized under these reaction conditions (Figure S2). Furthermore, *in situ* X-ray diffraction studies unequivocally showed that oxidized Co crystallized in the cubic CoO ($Fm\bar{3}m$) phase (Figure S3).

In view of the data gathered by XPS, we believe that metallic cobalt might be encapsulated by TiO_2 decreasing the overall number of active sites and thus the activity of the metallic Co/TiO_2. The wetting of small metallic particles by TiO_2 is well-known and was first reported by Tauster as a strong metal–support interaction (SMSI).[13−15] The reason for this encapsulation is not clear and might be related to the presence of specific adsorbates and/or thermally induced. No matter the reason, this Co/TiO_2 nanocomposite material possesses a surface dynamism which allows it to adapt to its environment. Figure S4 shows % Co on the surface of the Co/TiO_2 catalyst, as measured by AP-XPS under relevant conditions (100 mTorr O_2 or H_2) and lab XPS (Al K) for the fresh and spent catalysts after cycles of redox treatment and CO_2/H_2 reaction. It was

dx.doi.org/10.1021/ja412447q | J. Am. Chem. Soc. 2014, 136, 2260–2263

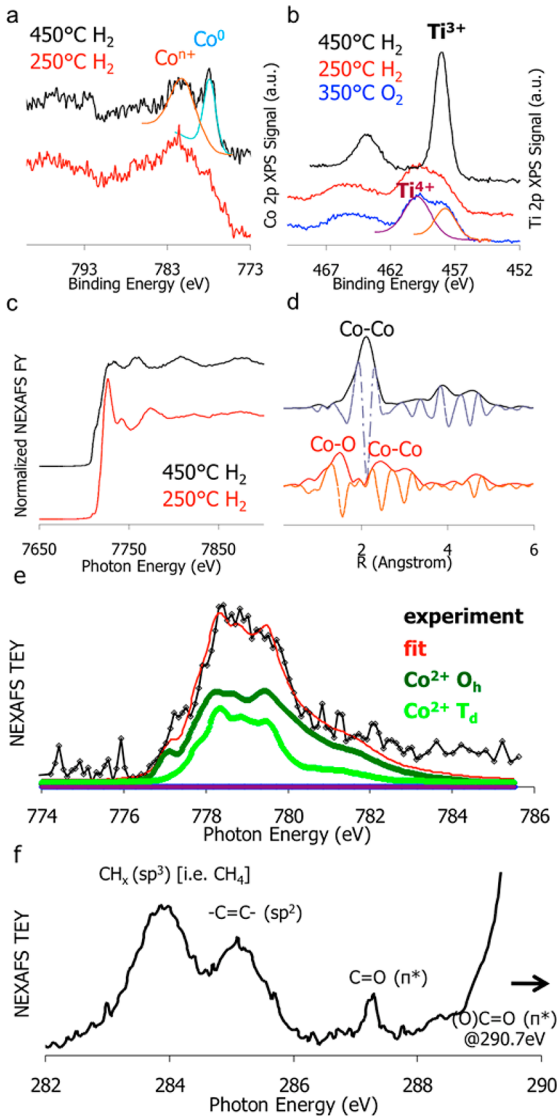

Figure 3. AP-XPS spectra of the Co/TiO_2 catalyst at (a) Co 2p and (b) Ti 2p core levels obtained under given conditions. *In situ* (c) NEXAFS spectrum and (d) the corresponding EXAFS oscillations at Co K absorption edge under given conditions. *In situ* NEXAFS TEY spectra at (e) Co L and (f) C K edges during reaction of CO_2/H_2 (1:3) at 1 atm and 250 °C. Least-square fitting in (e) was carried out using reference compounds as discussed in ref 17.

found that the % Co on the surface increased from 29 atom % in O_2 at 350 °C to 35 atom % in H_2 at 250 °C, suggestive of wetting of TiO_2 by CoO. Lab XPS evidenced that both the fresh and spent catalysts had approximately 30 atom % Co in the surface. At 450 °C in H_2, however, the % Co on the surface substantially dropped to 20 atom %. This is clearly reminiscent of reversible encapsulation of metallic Co,[15,16] present under these conditions, by TiO_{2-x} as a result of the lower surface free energy of the latter.[15] The possibility of $CoTiO_3$ formation has been considered; nonetheless, our AP-XPS, NEXAFS, and XRD data rule out the existence of such compounds at the surface or in the bulk.

In view of our findings, we believe that CoO forms a catalytically active and unique interface with TiO_2, which enhanced the activity of CO or CO_2 hydrogenation reactions with respect to metallic Co/TiO_2. Moreover, for both reactions the metallic Co/SiO_2 is less active than CoO/TiO_2. Our catalytic data demonstrate that a certain tuning of the product distribution could be achieved using metal/metal oxide support interaction.

■ ASSOCIATED CONTENT

Supporting Information

Contains the experimental protocols; TEM, HR-TEM, and HAADF images; STEM/EDS spectral maps as well as the *in situ* EXAFS FY spectra and XRD patterns obtained during CO_2/H_2 reaction. This material is available free of charge via the Internet at http://pubs.acs.org.

■ AUTHOR INFORMATION

Corresponding Authors

salayoglu@lbl.gov
somorjai@berkeley.edu

Notes

The authors declare no competing financial interest.

■ ACKNOWLEDGMENTS

This work was supported by the Director, Office of Basic Energy Sciences, Materials Sciences and Engineering Division, U.S. Department of Energy, under Contract DE-AC02-05CH11231. The user project at the Advanced Light Source and the Molecular Foundry at the Lawrence Berkeley National Laboratory was supported by the Director, Office of Science, Office of Basic Energy Sciences, U.S. Department of Energy, under Contract DE-AC02-05CH11231. Finally, Cheng-Shiuan Li is thanking Green Energy and Environment Research Laboratories, Industrial Technology Research Institute (Hsin-chu, Taiwan) for his research grant.

■ REFERENCES

(1) Bezemer, G. L.; Bitter, J. H.; Kuipers, H. P.; Oosterbeek, H.; Holewijn, J. E.; Xu, X.; Kapteijn, F.; van Dillen, A. J.; de Jong, K. P. *J. Am. Chem. Soc.* **2006**, *128*, 3956−3964.

(2) den Breejen, J. P.; Radstake, P. B.; Bezemer, G. L.; Bitter, J. H.; Frøseth, V.; Holmen, A.; de Jong, K. P. *J. Am. Chem. Soc.* **2009**, *131*, 7197−7203.

(3) Fischer, N.; van Steen, E.; Claeys, M. *J. Catal.* **2013**, *299*, 67−80.

(4) van Steen, E.; Claeys, M.; Dry, M. E.; van de Loosdrecht, J.; Viljoen, E. L.; Visagie, J. L. *J. Phys. Chem. B* **2005**, *109*, 3575−3577.

(5) Reuel, R. C.; Bartholomew, C. H. *J. Catal.* **1984**, *85*, 63−77.

(6) Iablokov, V.; Beaumont, S. K.; Alayoglu, S.; Pushkarev, V. V.; Specht, C.; Gao, J.; Alivisatos, A. P.; Kruse, N.; Somorjai, G. A. *Nano Lett.* **2012**, *12*, 3091−3096.

(7) An, K.; Alayoglu, S.; Musselwhite, N.; Plamthottam, S.; Melaet, G.; Lindeman, A. E.; Somorjai, G. A. *J. Am. Chem. Soc.* **2013**, *135*, 16689−16696.

(8) Schmidt-Winkel, P.; Lukens, W. W.; Yang, P.; Margolese, D. I.; Lettow, J. S.; Ying, J. Y.; Stucky, G. D. *Chem. Mater.* **2000**, *12*, 686−696.

(9) Seah, M. P.; Dench, W. A. *Surf. Interface Anal.* **1979**, *1*, 2−11.

(10) Cats, K. H.; Gonzalez-Jimenez, I. D.; Liu, Y.; Nelson, J.; van Campen, D.; Meirer, F.; van der Eerden, A. M.; de Groot, F. M.; Andrews, J. C.; Weckhuysen, B. M. *Chem. Commun. (Camb)* **2013**, *49*, 4622−4624.

(11) Tsakoumis, N. E.; Dehghan, R.; Johnsen, R. E.; Voronov, A.; van Beek, W.; Walmsley, J. C.; Borg, Ø.; Rytter, E.; Chen, D.; Rønning, M. *Catal. Today* **2013**, *205*, 86−93.

(12) Laffon, C.; Lasne, J.; Bournel, F.; Schulte, K.; Lacombe, S.; Parent, P. *Phys. Chem. Chem. Phys.* **2010**, *12*, 10865−10870.

(13) Tauster, S. J.; Fung, S. C.; Garten, R. L. *J. Am. Chem. Soc.* **1978**, *100*, 170−175.

(14) Tauster, S. J.; Fung, S. C.; Baker, R. T.; Horsley, J. A. *Science* **1981**, *211*, 1121−1125.
(15) Fu, Q.; Wagner, T. *Surf. Sci. Rep.* **2007**, *62*, 431−498.
(16) O'Shea, V. A.; Galván, M. C.; Prats, A. E.; Campos-Martin, J. M.; Fierro, J. L. *Chem. Commun. (Camb)* **2011**, *47*, 7131−7133.
(17) Zheng, F.; Alayoglu, S.; Guo, J.; Pushkarev, V.; Li, Y.; Glans, P. A.; Chen, J. L.; Somorjai, G. *Nano Lett.* **2011**, *11*, 847−853.